Research Paper

Exogenous Microparticles of Iron Oxide Bind to Activated Endothelial Cells but, Unlike Monocytes, Do Not Trigger an Endothelial Response

Andrew Jefferson, Neil Ruparelia and Robin P Choudhury ✉

Department of Cardiovascular Medicine and Oxford Acute Vascular Imaging Centre, University of Oxford, John Radcliffe Hospital, Oxford, OX3 9DU, United Kingdom.

✉ Corresponding author: Professor Robin P. Choudhury, Department of Cardiovascular Medicine, Level 6, West Wing, John Radcliffe Hospital, Oxford. OX3 9DU. Tel: +44-1865-234664 Fax: +44-1865-234667 E-mail: robin.choudhury@cardiov.ox.ac.uk.

Abstract

Targeting particles to sites of inflammation is of considerable interest for applications relating to molecular imaging and drug delivery. We and others have described micron-sized particles of iron oxide (MPIO) that can be directed using specific ligands (e.g. antibodies, peptides and oligosaccharides) to bind to mediators of vascular inflammation *in vivo*. Since leukocyte binding to these molecules can induce changes in the target cell, an outstanding question has been whether the binding of imaging particles to these mediators induces biologically significant changes in the endothelial cells, potentially initiating or propagating inflammation. Here, we address these questions by looking for changes in endothelial cells following binding of contrast agent. Specifically, we have quantified calcium flux, rearrangement of the actin cytoskeleton, production of reactive oxygen species (ROS), apoptosis and potential secondary changes, such as changes in gene and protein expression follow binding events to primary endothelial cells *in vitro*.

Although leukocytes induced changes to endothelial cell function, we did not see any significant changes to endothelial calcium flux, cytoskeletal organisation, production of ROS or induction of apoptosis in response to antibody-MPIO binding. Furthermore, there were no changes to gene expression monitored via real-time RT-PCR or presentation of protein on the cell surface measured using flow cytometry.

Our experiments demonstrate that whilst antibody-targeted microparticles mimic the binding capability of leukocytes to inflamed endothelium, they do not trigger the same cellular responses and do not appear to initiate or compound inflammation. These properties are desirable for targeted therapeutic and diagnostic agents.

Key words: Molecular Imaging, Inflammation, Microparticles

Introduction

Since the original description of McAteer *et al.*[1], targeted micron-size range particles of iron oxide have been applied for molecular imaging in experimental models of important human disease including multiple sclerosis[2, 3], cerebral metastases[4], epilepsy[5], ischemia reperfusion injury[6, 7] and atherosclerosis.[8, 9] Targeted contrast agents typically consist of a contrast element that imparts sensitivity for detection by a particular imaging modality and a targeting element, that is often an antibody or other molecule that confers specificity and binding affinity for the target of choice. Furthermore, particle-based

approaches have been proposed for the delivery of therapeutic agents, including drugs and miRNAs.[10, 11]

For the purposes outlined above, particles have been designed to bind to molecules that are differentially upregulated on activate endothelium, such as E-selectin, P-selectin and VCAM-1. These agents have been termed leukocyte-mimetic since their localisation relies on the binding to molecules that are crucial in leukocyte recruitment.

However, particle binding to functional, molecules expressed on the vascular endothelium has the potential to trigger cell signalling pathways and could even induce or compound inflammation at a tissue level. For instance, intercellular adhesion molecule-1 (ICAM-1), which is highly expressed in inflamed tissue *in vivo*,[12] plays a key role in endothelial cell response to leukocyte binding. Interactions between ICAM-1 and the leukocyte antigens αM/β2 (Mac-1) and α1/β2 (LFA-1) are responsible for leukocyte adhesion and spreading on the endothelium.[13, 14] ICAM-1 clustering as a result of leukocyte binding promotes release of intra-cellular calcium[15], activation of RhoA[16] and the formation of actin stress filaments.[17] Stress filaments form docking structures at the site of leukocyte binding and have also been reported to form a cup structure around 5 μm beads bound to the surface of an activated endothelial cell.[18] Less is known about signalling pathways originating via interaction of VCAM-1 with VLA-4, although it has been postulated that ligation of VCAM-1 with specific antibodies may induce similar cytoskeletal rearrangements to that seen when cross-linking ICAM-1.[17] Cross-linking of VCAM-1 by means of specific antibody-labelled 9.9 μm beads activated endothelial cell NADPH oxidase to generate reactive oxygen species (ROS).[19] In turn, ROS oxidise and stimulate protein kinase C (PKC) activity.[19] E-selectin mediated responses appear to be via protein clustering and localisation to components of the actin cytoskeleton, including α-actinin, filamin, vinculin, paxillin and functional adhesion kinase.[20] The role of E-selectin in endothelial signalling has been long-established, with anti-E-selectin antibodies capable of inducing changes to human umbilical vein endothelial cells (HUVEC)[21]; later work revealing E-selectin mediated phosphorylation and activation of MAP Kinase.[22]

As targeted microparticles are used more widely and have been proposed for human use[23], it is important to determine their effects on endothelial function. Accordingly, we report the effects of antibody-targeted microparticles (directed against endothelial E-selectin and VCAM-1[24]) on endothelial cells *in vitro.* Specifically, we have investigated whether particle binding induces changes to cellular calcium flux, production of reactive oxygen species, cytoskeletal rearrangement, gene expression levels and surface expression of molecular markers of inflammation. We compare the effects of MPIO *vs.* leukocyte binding on these processes.

Methods

Cell culture

Primary human aortic endothelial cells (HAEC) and human umbilical vein endothelial cells (HUVEC) (Invitrogen, Paisley, UK) were cultured in Medium 200 supplemented with Low-Serum Growth Supplement (LSGS) (Invitrogen). Cells were used between passages 2 and 4 and, when required, stimulated with recombinant human tumour necrosis factor-α (TNF-α, 10 ng mL^{-1}.) (Invitrogen) The human acute monocytic leukemia cell line (THP-1) was used as a positive biological control; cells were grown in RMPI-1640 medium supplemented with 10% FBS Gold (PAA Laboratories, Yeovil, UK) and 2 mM L-glutamine. When used as a positive control, THP-1 cells were centrifuged to remove culture medium, washed briefly in 1 x PBS and resuspended in LSGS-supplemented Medium 200 prior to adding to endothelial cells at a concentration of 1 x 10^5 cells mL^{-1} in all experiments.

Antibody-MPIO conjugation and handling

Mouse anti-human monoclonal antibodies against VCAM-1 (Clone 4B2), E-selectin (5D11) and ICAM-1 (BBIG-I1) (R&D Systems, Abingdon, UK) (25 μg of E-selectin and VCAM-1 antibody for E+V-MPIO, and 50 μg of ICAM-1 antibody for ICAM-1-MPIO) were covalently conjugated to ≈1.25 x 10^9, 1 μm-diameter tosyl-activated Dynalbeads (MPIO) (Invitrogen) as previously described.[1] The efficiency of the conjugation reaction is estimated to be >90% based on protein quantification assays taken before and after labelling. Antibody-MPIO were added to endothelial cells in all experiments at a concentration of 10 μg mL^{-1} antibody; ~ 2.5 x 10^8 MPIO mL^{-1}. Prior to adding to endothelial cells, antibody-MPIO suspensions were thoroughly vortexed and briefly sonicated to ensure a mono-dispersed suspension of particles and to limit clumping. Antibody-MPIO bind to cells either as separate, individual particles or small clumps which are limited to no more than approximately 5 particles.

Calcium imaging

HAEC grown in 35 mm culture dishes were stimulated with TNF-α for 7 hours and loaded with the fluorescent calcium indicator Fluo-4 (Invitrogen) as per the manufacturer's instructions for 1 hour at 37°C. Calcium responses to antibody-MPIO binding

under shear stress was performed by mounting culture dishes on a parallel-plate flow chamber (GlycoTech, Gaithersburg, USA) fitted with gasket B (0.25 cm x 0.025 cm) and connected to a syringe infusion pump (Pump 22; Harvard Apparatus, Cambridge, USA) and set to generate a shear stress over the cells of 1 dyne cm^{-2}. MPIO and THP-1 cells were also fluorescently labelled to allow differential detection; MPIO were labelled in suspension by incubating with 10 µg mL^{-1} goat anti-mouse Alexa Fluor 594 (Invitrogen) antibody for 30 minutes at 37°C and THP-1 cells were stained with the nuclear stain Hoechst 33342 (Invitrogen) at 2 µg mL^{-1} for 30 minutes then washed and resuspended in Medium 200 prior to running through the flow chamber. An Olympus IX-71 inverted microscope fitted with a 20x, 0.4 NA objective (Olympus UK, Southend-on-Sea, UK), and a QICAM cooled monochrome CCD camera (QImaging, Surrey, Canada) driven using ImagePro-Plus (Media Cybernetics, Bethesda, USA) were used for imaging. Fluo-4 fluorescence intensity was monitored for 3 minutes post-MPIO binding to a cell.

Reactive oxygen species assay

TNF-α stimulated and basal HAEC and HUVEC were incubated with 0.05% (wt/vol) nitroblue tetrazolium for 15 minutes prior to adding E+V-MPIO, ICAM-1-MPIO or THP-1 cells. Cells were briefly washed with 1 x PBS and then fixed for 5 minutes in methanol at room temperature. The production of reactive oxygen species was assessed by looking for the formation of intracellular formazan precipitate using a 40x 0.6 NA objective. One hundred cells for each experiment were scored for the presence or absence of formazan.

Cytoskeletal rearrangements

HAEC and HUVEC grown on poly-d-lysine coated glass were stimulated with TNF-α for 6 hours, and incubated with E+V-MPIO, ICAM-1-MPIO or THP-1 cells for a further 2 hours. Cells were washed with PBS and fixed in methanol-free formaldehyde 4 % for 10 minutes at room temperature. Phalloidin-TRITC (Invitrogen) was used to stain F-actin. After a final wash in PBS, coverslips were mounted on a standard microscope slide in *SlowFade* Gold antifade reagent with 4',6-diamidino-2-phenylindole (Invitrogen). Images were taken using a 100x 1.3 NA oil immersion objective fitted to the microscope detailed above.

RNA Extraction and RT-PCR

Quantitative real-time RT-PCR was used to measure expression of VCAM-1 (CD106), E-selectin (CD62E) and ICAM-1 (CD54) in HAEC and HUVEC under basal and stimulated conditions following binding of E+V-MPIO, ICAM-1-MPIO or THP-1 cells. GAPDH was used as a normalization gene. Following stimulation with TNF-α for 2 hours, targeted MPIO and THP-1 cells were added and incubated for a further 2 hours. RNA was extracted using an RNeasy Mini Kit (Qiagen, Crawley, UK) and cDNA was synthesised using a QuantiTect reverse transcription kit (Qiagen). TaqMan™ primers for VCAM-1, E-selectin, PECAM-1 and GAPDH were used to amplify cDNA on a StepOne PCR system (Applied Biosystems, Warrington, UK). Relative quantities of mRNA expressed in arbitrary units were calculated using the $2^{\Delta\Delta Ct}$ method.[25]

Flow cytometry to establish relative ligand abundance

HAEC and HUVEC were stimulated with TNF-α for 6 hours, and incubated with E+V-MPIO, ICAM-1-MPIO or THP-1 cells for a further 2 hours. Following washing with PBS cells were detached using non-enzymatic cell dissociation solution (Sigma, Poole, UK). The cells were centrifuged (1200 rpm; 5 minutes) and resuspended in 100 µL PBS. Mouse anti-human E-Selectin antibody was added at a final concentration of 10 µg mL^{-1}. Goat anti-mouse Alexa Fluor 488 (Invitrogen) was added at a concentration of 10 µg mL^{-1}. Flow cytometry experiments were performed on a CyAn flow cytometer and the data analysed using FlowJO software, version 7.6.3 (Tree Star Inc., Ashland, USA), gates of interest were set using unstained and IgG stained samples to control for background and autofluorescence.

Apoptosis assay

The effect of antibody-MPIO on cell viability and induction of apoptosis in endothelial cells was determined by staining with a FITC-conjugated Annexin-V antibody and Propidium Iodide (PI) to identify apoptotic and/or dead cells respectively, using an Annexin-V/Dead Cell Apoptosis Kit (Invitrogen). The kit was used in accordance with the manufacturer's protocol and cells analysed immediately after staining on a CyAn flow-cytometer as described above. Apoptosis was induced in HAEC and HUVEC as a positive control by serum starving cells for 4 hours prior to staining. To allow differentiation between endothelial and THP-1 cells in the relevant samples, THP-1 cells were loaded with Hoechst 33342 as described above, then washed prior to incubating with endothelial cells.

Results

Binding of THP-1 cells, but not E+V-MPIO induce calcium flux in aortic endothelial cells

Fluo-4 intensity was tracked over a 3 minute pe-

riod following MPIO or THP-1 binding to TNF-α stimulated HAEC. Binding of dual-targeted E+V-MPIO to cells (Figure 1A) did not result in changes to calcium concentration within the cells observed. Calcium flux was observed upon binding of THP-1 cells (Figure 1B); following binding, a slow increase in Fluo-4 intensity which peaked at around 60 seconds post-binding was observed before fluorescence normalised to baseline (Figure 1C).
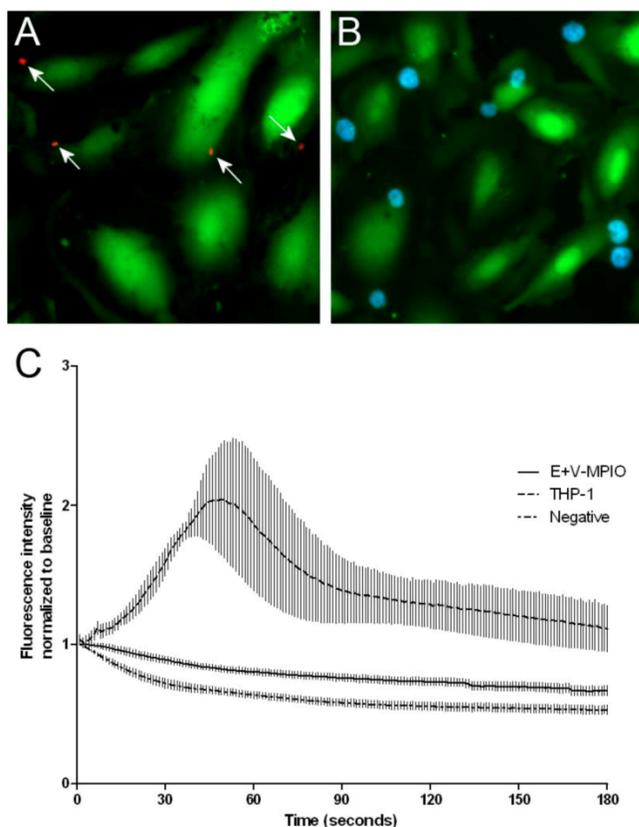
Fig 1. Stimulated HAEC were loaded with the fluorescent calcium indicator Fluo-4 to detect calcium flux following binding events. E+V-MPIO were separately labelled with an Alexa Fluor 594 antibody to allow visualisation following binding events (indicated by white arrows) (A). THP-1 cells were loaded with Hoechst 33342 to enable fluorescent visualisation following binding to endothelial cells (light blue) (B). E+V-MPIO, THP-1 or vehicle only were run across stimulated HAEC in a Glycotech parallel-plate flow chamber at 1 dyne cm^{-2} and fluorescence intensity was measured over a 3 minute period following a binding event (A & B; MPIO marked with arrows). The area of fluorescence measured did not include the newly-bound particle/cell to prevent measuring artefacts. The E+V-MPIO and negative control showed a gradual decrease in Fluo-4 intensity over time due to photobleaching (C). However upon binding of THP-1 cells to HAEC, there was an increase in cellular calcium detected via an increase in fluorescence intensity which peaked at approximately 60 seconds post-binding and which returned near to baseline in the subsequent 2 minutes.

Targeted MPIO binding to endothelial cells does not result in the production of reactive oxygen species

The production of reactive oxygen species (ROS) in endothelial cells in response to antibody-MPIO binding was investigated using nitroblue tetrazolium (NBT), which in the presence of ROS is reduced to formazan, a black, insoluble intracellular precipitate. Cells incubated with NBT were then incubated with E+V-MPIO and ICAM-1-MPIO, and a positive control of ascorbic acid. Representative images taken without phase contrast for clarity of MPIO and formazan precipitate are shown for HAEC (Figure 2A-D) and HUVEC (Figure 2E-H). Scoring cells for presence or absence of formazan (Figure 2I) revealed a low percentage of positive HAEC and HUVEC when incubated with E+V- and ICAM-1-MPIO and negative controls, none of which were statistically different (P > 0.05 in all instances), but a significantly higher count in the ascorbic acid positive control (P = 0.0001). Incubating HAEC and HUVEC with the corresponding antibody-only controls also resulted in a low percentage of formazan-positive cells, with no significant difference from the negative control (P > 0.05 in all instances) (data not shown).

Endothelial cytoskeleton is reorganised upon exposure to THP-1 cells but not with targeted MPIO

Confocal analysis of phalloidin-stained endothelial cells revealed no difference between cells incubated with E+V-MPIO and ICAM-1-MPIO, and negative controls, with a fine network of stress fibres running through the cells, as is characteristic for cells cultured on glass. However, when incubating endothelial cells with THP-1 macrophages, F-actin filaments were bundled at the site of binding. Z-stacks were obtained and flat projections generated for HAEC incubated with E+V-MPIO (Figure 3A), negative control (Figure 3B) and THP-1 (Figure 3C). Inserts show a side-on view generated with a 3D projection of image slices. Transverse line profiles (shown on images) reveal a characteristic pattern in E+V-MPIO and negative cells, with a clearly different profile - representing peripheral bundling - observed in THP-1-treated cells. Classifying F-actin organisation as either "fine filaments" or "bundled filaments" further corroborates the image findings, with a large proportion of HAEC and HUVEC having bundled filaments when treated with THP-1 cells, but not with E+V-MPIO, ICAM-1-MPIO or antibody-alone controls (Figure 3D&E).
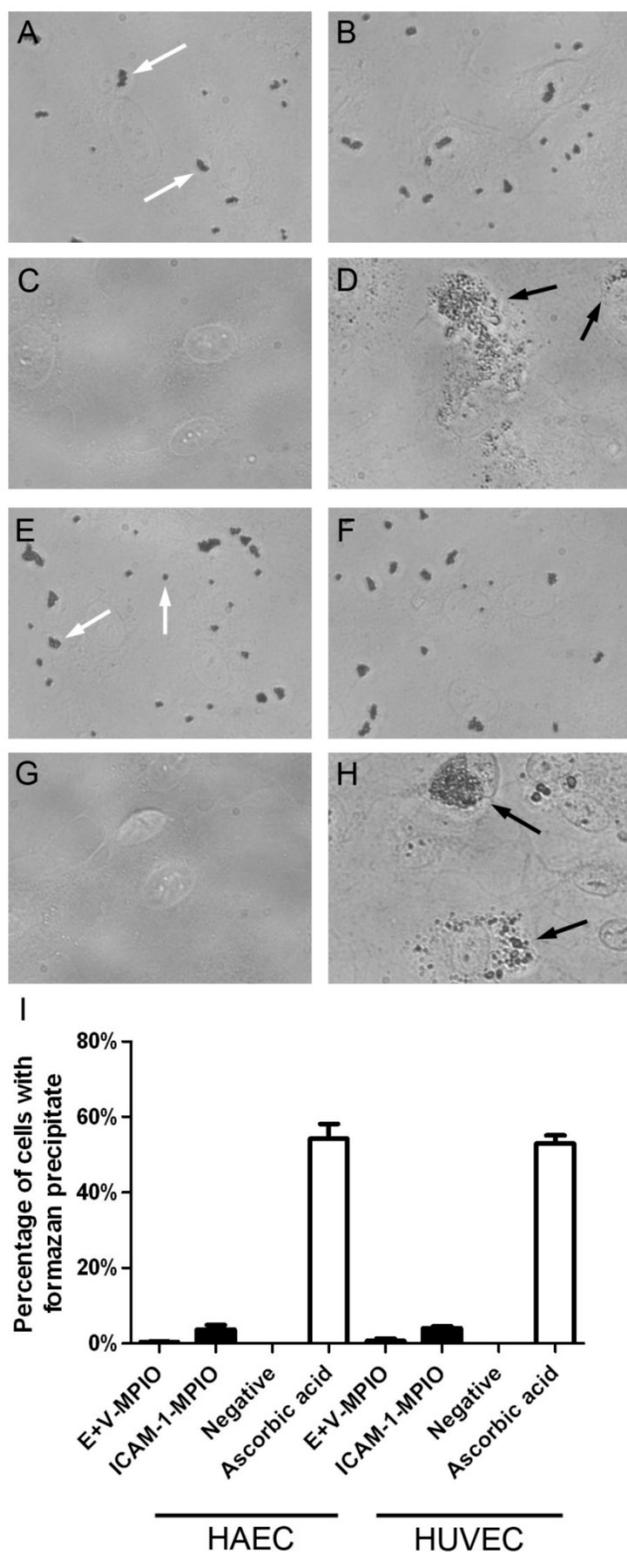
Fig 2. The production of ROS following binding events was assessed by loading cells with nitroblue tetrazolium and looking for the reduction product formazan via light microscopy. In HAEC (A-C) and HUVEC (E-G) treated with E+V-MPIO, ICAM-1-MPIO (MPIO indicated with white arrows) and medium-only very few cells contained formazan precipitate. Approximately 50% of both cell types treated with ascorbic acid (D&H) contained formazan precipitate (precipitate indicated with black arrows to allow distinction between MPIO and precipitate). Scoring of cells for presence or absence of formazan precipitate revealed no significant difference between MPIO-treated and negative controls (I).

Antibody-MPIO binding does not induce changes to gene expression of inflammatory markers

Expression of E-selectin, VCAM-1 and ICAM-1 mRNA was assessed in TNF-α stimulated and basal HAEC and HUVEC incubated with E+V-MPIO and ICAM-1-MPIO, and THP-1 macrophages. In all stimulated samples, there was no statistically significant difference in expression of any of the genes tested between samples incubated with the antibody-MPIO, THP-1 cells or negative (vehicle only) controls (P > 0.05 for all comparisons) (Figure 4A-F).

In the basal (unstimulated) samples, minimal expression of all genes was measured in the antibody-MPIO samples and negative samples. Upregulation of all genes was observed in basal endothelial cells treated with THP-1 macrophages. Contribution of THP-1 RNA towards expression data was accounted for by extracting RNA from THP-1 cells in isolation and testing for expression of E-selectin, VCAM-1 and ICAM-1; no gene expression was detected (data not shown).

Antibody-MPIO binding does not induce changes to the surface density of inflammatory markers on endothelial cells

The surface density of E-selectin, as a representative surface marker of inflammation, was assessed in stimulated and basal HAEC and HUVEC incubated with antibody-MPIO and THP-1 cells using flow cytometry. No significant differences were observed in the geometric mean fluorescence intensity of cells incubated with E+V-MPIO and ICAM-1-MPIO when compared with negative controls (P > 0.05 for all comparisons) (Figure 5A & B).

Antibody-MPIO binding does not induce apoptosis or affect endothelial cell viability

Annexin-V and PI staining of endothelial cells was used to look for induction of apoptosis and cell death following antibody-MPIO binding. Apoptosis was not induced in stimulated and basal HAEC and HUVEC incubated with MPIO and THP-1 cells, with no significant differences observed in the fold-change in numbers of apoptotic (Annexin V$^+$/PI$^-$) cells when compared with negative controls (P > 0.05 for all comparisons) (Figure 6A, B & C). A significant difference was observed however when comparing experimental conditions in stimulated HAEC and HUVEC with the positive controls of serum starvation to induce apoptosis (P ≤ 0.05 for all comparisons). Furthermore, no significant difference in the percentage of dead cells (Annexin V$^+$/PI$^+$) was observed between MPIO, THP-1 and negative controls (P > 0.05 for all comparisons) (data not shown).
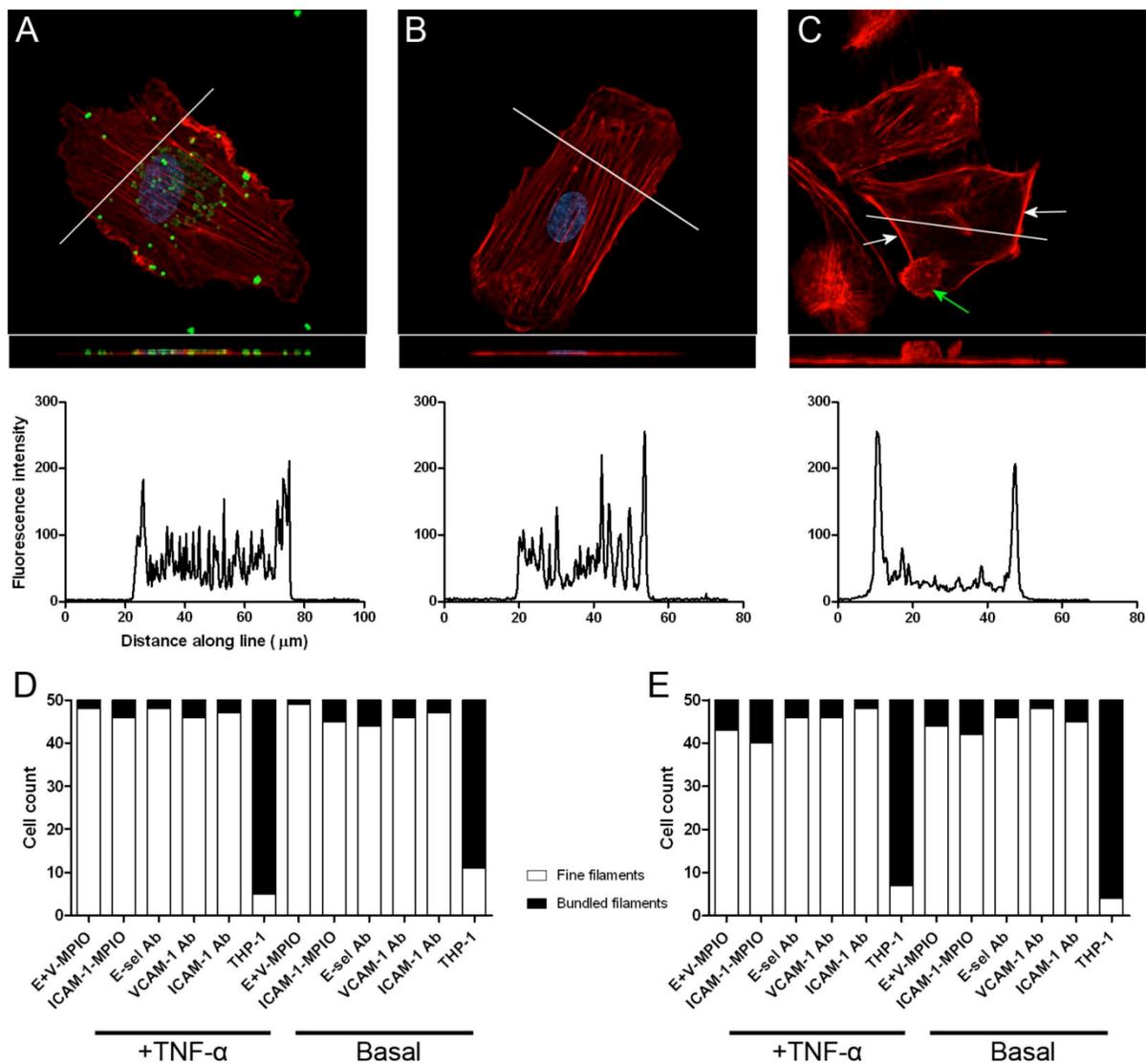
Fig 3. Phalloidin-TRITC was used to stain F-actin filaments to assess the morphology of the endothelial cytoskeleton via laser scanning confocal microscopy. Images are single-plane projections generated by taking Z-stacks, with side-on projections also presented as inlays. No large-scale changes to actin organisation were seen when E+V-MPIO bound to stimulated HAEC, nor in negative controls (A & B). Upon binding of THP-1 to stimulated HAEC, F-actin becomes bundled and is redistributed at the edges of cells and at sites of THP-1 binding (C). Line profiles drawn across cells demonstrate different cross sectional staining in cells treated with THP-1 cells. Classification of F-actin filaments as "fine" or "bundled" shows no difference between cells with MPIO and antibody-only bound and negatives, but a marked difference when THP-1 cells have bound (D & E).
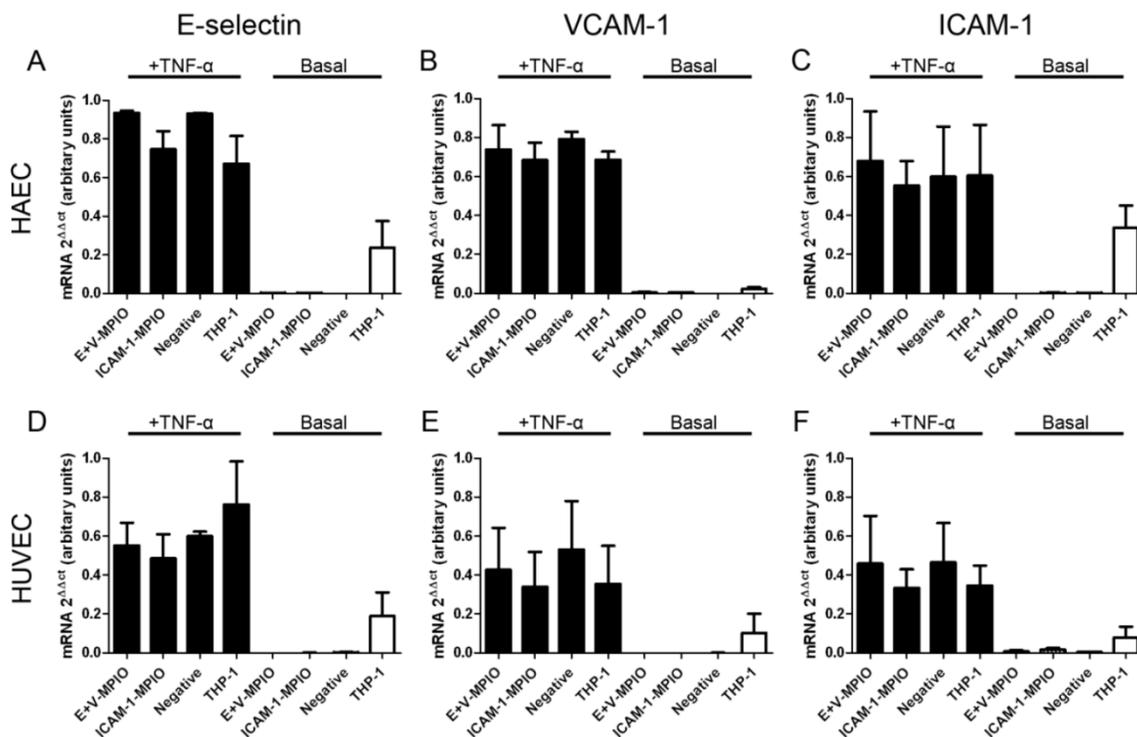
Fig 4. Real-time RT-PCR was used to assess expression of E-selectin (A & D), VCAM-1 (B & E) and ICAM-1 (C & F) in stimulated (black columns) and basal (white columns) HAEC and HUVEC respectively incubated with E+V- and ICAM-1-MPIO, and THP-1 cells. In all stimulated cells, there were no differences between any of the treatments (P>0.05 in all comparisons). In basal HAEC and HUVEC, binding of THP-1 cells induced expression of all genes tested.

Fig 5. Flow cytometry to assess the relative surface density of E-selectin on stimulated (+) and basal (-) HAEC and HUVEC treated with MPIO and THP-1 cells. E-selectin was expressed on the surface of stimulated HAEC (A) and HUVEC (B), with no significant difference between MPIO-treated and non-treated cells (P>0.05). The apparent reduction in E-selectin density in cells incubated with THP-1 may be due to masking of E-selectin by bound THP-1 cells.
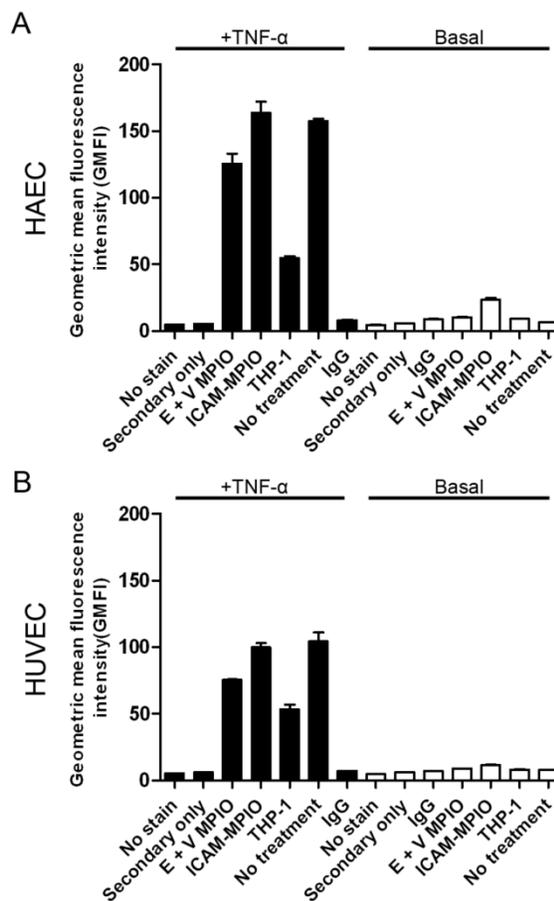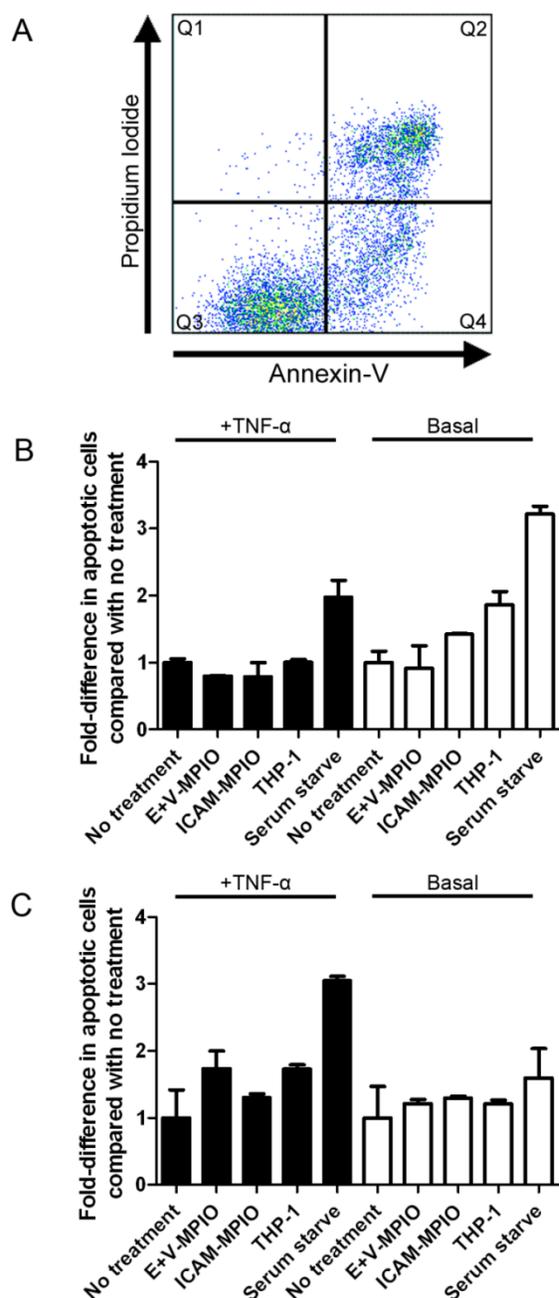
Fig 6. Flow cytometry of Annexin-V/Propidium Iodide-stained endothelial cells was used to assess induction of apoptosis following binding of antibody-MPIO. The flow cytometry plot (A) divides cells into 3 main groups; live cells (Annexin-V⁻/PI⁻) are represented in Q3, live but apoptotic cells (Annexin-V⁺/PI⁻) in Q4 and apoptotic dead cells (Annexin-V⁺/PI⁺) in Q2. When looking at fold change in apoptosis, binding of E+V-MPIO and ICAM-1-MPIO did not induce apoptosis in stimulated and basal HAEC and HUVEC (B & C).

Discussion

Targeted particles that bind to sites of endothelial activation are of considerable interest as imaging contrast agents[1-6, 9, 26] and for the local delivery of drugs[10] and genes.[11] Leukocyte binding to acti-

vated endothelium provokes a variety of responses in the endothelial cell. Therefore, an important consideration for the development of endothelium-targeted agents towards clinically-usable products is whether their binding induces potentially detrimental effects in the target cell.

Here, we show that, in contrast to the response to monocyte binding, antibody-targeted MPIO binding to primary endothelial cells *in vitro* has no measurable effect on a range of biologically important processes. Specifically, particle binding did not promote calcium flux, production of ROS or cytoskeletal rearrangement – all of which occur shortly after leukocyte binding. These results indicate that, whilst mimicking some of the binding properties of leukocytes, which is desirable for localising to sites of disease, antibody targeted contrast agents recognising either E-selectin or VCAM-1 do not trigger endothelial signalling events that may activate or exacerbate inflammation. Furthermore, we demonstrate that our contrast agent does not induce apoptosis in the target endothelial cells.

We also examined what might be considered secondary changes to endothelial cell phenotype such as the expression of mRNA for the inflammatory mediators E-selectin, VCAM-1 and ICAM-1 and surface density of these markers. We did not identify any significant changes to these parameters with antibody-MPIO binding.

The inclusion of both basal-state and TNF-α stimulated cells was designed to identify whether our targeted contrast agent 1) stimulated basal cells and 2) compounded a pre-existing inflammatory stimulus. In neither case was there a significant change in endothelial cells treated with contrast agent. These findings have important ramifications for the use of such contrast agents *in vivo*, where switching-on and/or compounding inflammation would be undesirable consequences that would confound the molecular imaging and potentially modify / exacerbate the disease process.

The response of endothelial cells to leukocyte binding appears to be driven in part by endothelial ligand cross linking; in this instance, molecules far apart on the endothelial cell surface may be brought into close contact by the bound cell, thus inducing cellular responses.[15-17] Similar effects have been noted when using larger particles not dissimilar in size to that of cells to mimic the binding of leukocytes.[18, 19] However, in direct contrast to these studies, our choice of using smaller, 1 μm particles may be responsible for the absence of a detectable response. The smaller diameter of our particles might minimise the spatial effect of molecular cross-linking

of E-selectin, VCAM-1 and ICAM-1, which could account for the lack of cell response. Endothelial cell endocytosis of antibody-labelled MPIO does not appear to occur,[9] and thus the interaction between cells and particles is due to antibody-receptor interaction at the cell surface.

Conclusions

Antibody-based targeted microparticles of iron oxide do not appear to trigger signalling mechanisms in endothelial cells resulting in the phenotypic changes that are characterised upon the binding of leukocytes.

Acknowledgements

Competing Interests

The authors have declared that no competing interest exists.

References

1. McAteer MA, Sibson NR, von Zur Muhlen C, Schneider JE, Lowe AS, Warrick N, et al. In vivo magnetic resonance imaging of acute brain inflammation using microparticles of iron oxide. Nature medicine. 2007; 13: 1253-8.
2. Serres S, Mardiguian S, Campbell SJ, McAteer MA, Akhtar A, Krapitchev A, et al. VCAM-1-targeted magnetic resonance imaging reveals subclinical disease in a mouse model of multiple sclerosis. Faseb J. 2011; 25: 4415-22.
3. van Kasteren SI, Campbell SJ, Serres S, Anthony DC, Sibson NR, Davis BG. Glyconanoparticles allow pre-symptomatic in vivo imaging of brain disease. Proceedings of the National Academy of Sciences of the United States of America. 2009; 106: 18-23.
4. Serres S, Soto MS, Hamilton A, McAteer MA, Carbonell WS, Robson MD, et al. Molecular MRI enables early and sensitive detection of brain metastases. Proceedings of the National Academy of Sciences of the United States of America. 2012; 109: 6674-9.
5. Duffy BA, Choy M, Riegler J, Wells JA, Anthony DC, Scott RC, et al. Imaging seizure-induced inflammation using an antibody targeted iron oxide contrast agent. NeuroImage. 2012; 60: 1149-55.
6. Akhtar AM, Schneider JE, Chapman SJ, Jefferson A, Digby JE, Mankia K, et al. In vivo quantification of VCAM-1 expression in renal ischemia reperfusion injury using non-invasive magnetic resonance molecular imaging. PLoS One. 2010; 5: e12800. doi:10.1371/journal.pone.0012800.
7. Grieve SM, Lonborg J, Mazhar J, Tan TC, Ho E, Liu CC, et al. Cardiac magnetic resonance imaging of rapid VCAM-1 up-regulation in myocardial ischemia-reperfusion injury. Eur Biophys J. 2012.
8. McAteer MA, Mankia K, Ruparelia N, Jefferson A, Nugent HB, Stork LA, et al. A leukocyte-mimetic magnetic resonance imaging contrast agent homes rapidly to activated endothelium and tracks with atherosclerotic lesion macrophage content. Arteriosclerosis, thrombosis, and vascular biology. 2012; 32: 1427-35.
9. McAteer MA, Schneider JE, Ali ZA, Warrick N, Bursill CA, von zur Muhlen C, et al. Magnetic resonance imaging of endothelial adhesion molecules in mouse atherosclerosis using dual-targeted microparticles of iron oxide. Arteriosclerosis, thrombosis, and vascular biology. 2008; 28: 77-83.
10. Das M, Mishra D, Dhak P, Gupta S, Maiti TK, Basak A, et al. Biofunctionalized, phosphonate-grafted, ultrasmall iron oxide nanoparticles for combined targeted cancer therapy and multimodal imaging. Small (Weinheim an der Bergstrasse, Germany). 2009; 5: 2883-93.
11. Pan Y, Zhang Y, Jia T, Zhang K, Li J, Wang L. Development of a microRNA delivery system based on bacteriophage MS2 virus-like particles. The FEBS journal. 2012; 279: 1198-208.
12. Mulligan MS, Vaporciyan AA, Miyasaka M, Tamatani T, Ward PA. Tumor necrosis factor alpha regulates in vivo intrapulmonary expression of ICAM-1. The American journal of pathology. 1993; 142: 1739-49.
13. Diamond MS, Staunton DE, de Fougerolles AR, Stacker SA, Garcia-Aguilar J, Hibbs ML, et al. ICAM-1 (CD54): a counter-receptor for Mac-1 (CD11b/CD18). The Journal of cell biology. 1990; 111: 3129-39.
14. Makgoba MW, Sanders ME, Ginther Luce GE, Dustin ML, Springer TA, Clark EA, et al. ICAM-1 a ligand for LFA-1-dependent adhesion of B, T and myeloid cells. Nature. 1988; 331: 86-8.
15. Clayton A, Evans RA, Pettit E, Hallett M, Williams JD, Steadman R. Cellular activation through the ligation of intercellular adhesion molecule-1. Journal of cell science. 1998; 111 (Pt 4): 443-53.
16. Etienne S, Adamson P, Greenwood J, Strosberg AD, Cazaubon S, Couraud PO. ICAM-1 signaling pathways associated with Rho activation in microvascular brain endothelial cells. J Immunol. 1998; 161: 5755-61.
17. Millan J, Ridley AJ. Rho GTPases and leucocyte-induced endothelial remodelling. The Biochemical journal. 2005; 385: 329-37.
18. van Buul JD, Kanters E, Hordijk PL. Endothelial signaling by Ig-like cell adhesion molecules. Arteriosclerosis, thrombosis, and vascular biology. 2007; 27: 1870-6.
19. Deem TL, Abdala-Valencia H, Cook-Mills JM. VCAM-1 activation of endothelial cell protein tyrosine phosphatase 1B. J Immunol. 2007; 178: 3865-73.
20. Yoshida M, Westlin WF, Wang N, Ingber DE, Rosenzweig A, Resnick N, et al. Leukocyte adhesion to vascular endothelium induces E-selectin linkage to the actin cytoskeleton. The Journal of cell biology. 1996; 133: 445-55.
21. Kaplanski G, Farnarier C, Benoliel AM, Foa C, Kaplanski S, Bongrand P. A novel role for E- and P-selectins: shape control of endothelial cell monolayers. Journal of cell science. 1994; 107 (Pt 9): 2449-57.
22. Hu Y, Kiely JM, Szente BE, Rosenzweig A, Gimbrone MA, Jr. E-selectin-dependent signaling via the mitogen-activated protein kinase pathway in vascular endothelial cells. J Immunol. 2000; 165: 2142-8.
23. McAteer MA, Akhtar AM, von Zur Muhlen C, Choudhury RP. An approach to molecular imaging of atherosclerosis, thrombosis, and vascular inflammation using microparticles of iron oxide. Atherosclerosis. 2010; 209: 18-27.
24. Jefferson A, Wijesurendra RS, McAteer MA, Digby JE, Douglas G, Bannister T, et al. Molecular imaging with optical coherence tomography using ligand-conjugated microparticles that detect activated endothelial cells: rational design through target quantification. Atherosclerosis. 2011; 219: 579-87.
25. Pfaffl MW. A new mathematical model for relative quantification in real-time RT-PCR. Nucleic acids research. 2001; 29: e45.
26. von Zur Muhlen C, von Elverfeldt D, Choudhury RP, Ender J, Ahrens I, Schwarz M, et al. Functionalized magnetic resonance contrast agent selectively binds to glycoprotein IIb/IIIa on activated human platelets under flow conditions and is detectable at clinically relevant field strengths. Mol Imaging. 2008; 7: 59-67.